

# A Cooperative Multi-Satellite Mission for Controlled Active Debris Removal from Low Earth Orbit

Bogdan Udrea  
 VisSidus Technologies, Inc.  
 Daytona Beach, FL 32114  
 206-227-8075  
 bogdan.udrea@vissidus.com

Mikey Nayak  
 RedSky Research  
 Albuquerque, NM 87117  
 386-983-6135  
 nayak@redskyresearch.org

**Abstract**—This paper presents the concept of operations and preliminary design of a multi-satellite mission for the active removal of large pieces of debris from low Earth orbit. The mission consists of a mothership minisatellite, that carries six nanosatellites. The mothership acquires a relative orbit of a few kilometers with respect to the piece of orbital debris of interest and determines the attitude state of the debris and good docking locations for the nanosatellites. The nanosatellites deploy sequentially and dock with the piece of debris. Once all the nanosatellites are docked with the debris they cooperatively perform its structural analysis to determine safe maneuvering profiles for its detumble and deorbit. The mothership then docks with the piece of debris and applies maneuvers to deorbit it. Systems engineering budgets have been determined for the mass and propellant and a preliminary mission cost has been estimated. They are presented together with the functional architectures of each spacecraft and the results of mission design obtained with the Systems Tool Kit.

## TABLE OF CONTENTS

1	INTRODUCTION.....	1
2	ORBITAL DEBRIS REMOVAL BACKGROUND ....	2
3	TOP LEVEL MISSION REQUIREMENTS .....	2
4	CONCEPT OF OPERATIONS.....	2
5	FEASIBILITY ANALYSIS .....	5
6	MANEUVER DESIGN AND PLANNING .....	7
7	CONCLUSIONS .....	11
	APPENDICES .....	12
A	BENEFITS OF THE MISSION STUDY .....	12
B	UNDERSTANDING OF MAJOR CHALLENGES ....	12
	ACKNOWLEDGMENTS .....	13
	REFERENCES .....	13
	BIOGRAPHY .....	15

## 1. INTRODUCTION

Orbital debris is defined as all artificial objects in Earth orbit which no longer serve a useful purpose; i.e., inactive spacecraft, upper stages of launch vehicles also called rocket bodies (RBs), material released intentionally or unintentionally during stage separation, and material resulting from RB and satellite explosions and collisions. The danger that orbital debris poses to space activities has been demonstrated by the 10 Feb 2009 collision between the active Iridium 33 (US) satellite and the decommissioned Kosmos 2251 (Russia). Another telling example is the mission risk and operational burden on the crew and operators of the International Space Station (ISS) who dealt with six orbital debris events between

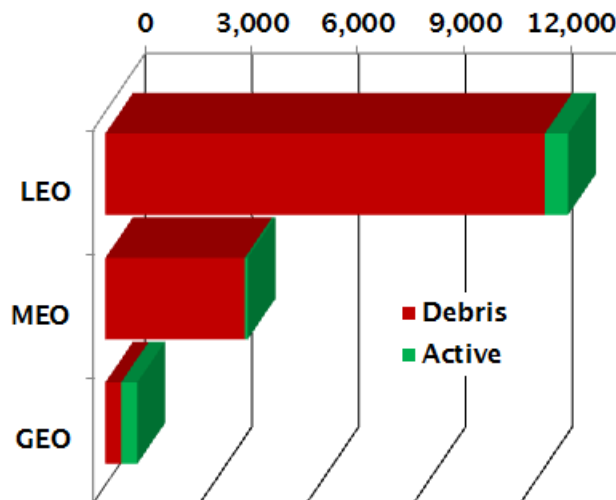


**Figure 1.** Distributions of orbital debris and active satellites in June 2014. LEO altitudes between 200 and 2,000 km, MEO altitudes between 2,000 and 35,586km, and GEO altitudes between 35,586 and 35,986 km.

Apr 2011 and Mar 2012. Four of the events resulted in the ISS performing collision avoidance maneuvers (CAMs) and two resulted in the crew retreating to the Soyuz capsules due to the lack of time to perform CAMs [1]. It is interesting to note that during 2013 the ISS performed no CAMs. Instead of considering it a sign of abating orbital debris threats to the ISS, NASA indicated that the quiet year reflects the chaotic nature of the [debris] population [2]. This statement has been reinforced by the fact that the ISS has performed three CAMs in 2014 [3] alone.

The altitude range with the largest number of tracked debris objects spans the low Earth orbits (LEOs), as shown in Figure 1. The number of active satellites in Figure 1 has been obtained from the Union of Concerned Scientists Satellite Database<sup>2</sup> which includes the launches through 31 July 2014. The number of total resident objects have been compiled by authors from multiple publicly available sources.

Mitigation measures, which are designed to either safely deorbit LEO satellites within 25 years [4] or passivate them after the end of their mission, have been implemented. However, to this date no remediation of orbital debris, or ADR, mission has flown. Liou [5] shows that, in the assumption that the mitigation success rate is 90% and ADR missions commence in 2020, at the rate of removing five large objects per year, the total number of objects in LEO will increase only slightly, from approximately 13,000 in 2010 to about 14,000 in 2210. The “business-as-usual” scenario [5] in which no

978-1-4799-5380-6/15/\$31.00 ©2015 IEEE.

<sup>1</sup> IEEEAC Paper #2095, Version 0.1, Updated 09/01/2015.

<sup>2</sup><http://www.ucsusa.org>

ADR missions are performed and the post-mission disposal is 90% results in doubling of the total number of objects in LEO by 2210 and reach about 22,000. As a consequence, the proposed concept focuses on the *controlled active removal* of large debris objects from LEO.

The goal of the work described here is the design of a mission architecture for cost-efficient, repeatable, and robust active debris removal (ADR) of large pieces of orbital debris and thus provide long-term sustainability of the space environment in LEO.

## 2. ORBITAL DEBRIS REMOVAL BACKGROUND

Kaplan [6] and Weeden [7] present a comprehensive survey of space debris removal methods which range from what could be called traditional, such as robotic capture, to the exotic such as use of laser ablation to generate deorbit forces. The most refined controlled ADR concept has been presented at the 3<sup>rd</sup> European Workshop on Orbital Debris Modeling and Remediation (16-18 June 2014) by Airbus Defence and Space (formerly Astrium) and it uses a cast net [8], [9]. The three main debris removal concepts pursued by Astrium rely on: 1) a robotic arm that grabs the tumbling target by matching its angular rates. Once in its grip, the ADR satellite detumbles the target and then performs reentry maneuvers; 2) a cast net that wraps around the target and it is then tightened with mechanisms in the weights of the cast net; 3) a harpoon that penetrates the target which is then reeled-in. Once the target is either captured by the net or grappled by the harpoon, the ADR satellite applies reentry maneuvers. In all three cases the capture mechanisms represent a single point of failure with highly uncertain contact dynamics. The deployment dynamics of the cast net and the harpoon concepts increase the level of uncertainty and also couple the attitude motion of the ADR satellite to that of its target through highly compliant structures. Last but not least the net and the harpoon have the potential of creating additional debris in the case of failure. A concept proposed by Castronuovo [10] borrows from the robot arm concept and uses a second robot arm on the ADR satellite to attach a deorbit module to the debris object.

Compared to the concepts described above, the *Curimba* mission shifts the emphasis from the highly uncertain dynamic coupling between a large ADR satellite and its target to relatively well understood dynamics of rendezvous and docking performed with small and physically robust nanosatellites.

A concept that bears the most similarity with the one described here is that of Astroscale [11] in which a mothership deploys passive kits of 20 kg that attach to the target using a sticky pad mounted on a ball joint. The kits employ solid rocket motors to perform deorbit maneuvers. For the Astroscale concept to be successful it is required that the target object attitude rate be below 2°/s about the major axis and the sticky pad to work on the first attempt.

Compared to the Astroscale concept the nanosatellites of the *Curimba* mission can perform multiple docking attempts to any spot on the target, independently of the direction of the angular rate vector of the target and are designed for target angular rates as large as 20°/s per axis. The active docking mechanism ensures the robustness of the docking in the presence of irregular surfaces and uncertain surface properties.

## 3. TOP LEVEL MISSION REQUIREMENTS

The casualty threshold requirement for the US missions is set both in DoD Instruction 3100.12 [4] and NASA-STD8719.14 [12] and states that the “risk from the total debris casualty area for components and structural fragments surviving reentry shall not exceed 1 in 10,000.” Bonnal et al. [13] quantify the risks presented by the reentry of large debris using a requirement in the French Law on Space Operations that specifies a maximum acceptable casualty risk, equal to that set by NASA and DoD, of 1 in 10,000 per space operation. According to [13], the requirement flows down to an ADR mission requirement that orbital debris with a mass higher than 500 kg shall be deorbited in a controlled manner. The Agena D RB has a dry mass of 673 kg and thus a mission designed to deorbit it must ensure that the casualty risk is below the required threshold. The assertion about the Agena D RB casualty risk has been validated and the results of the analysis are discussed below, in Section 5.

NASA-STD8719.14 also requires that the “selected [reentry] trajectory shall ensure that no surviving debris impact with a kinetic energy greater than 15 J is closer than 370 km from foreign landmasses, or is within 50 km from the continental U.S., territories of the U.S., and the permanent ice pack of Antarctica” which leads to the selection of a splashdown reentry.

In order to satisfy the requirements discussed above *Curimba* is a controlled ADR mission. This means that the mission should gain control of the attitude motion of the target RB with the purpose of stabilizing it and maintain attitude control during the application of reentry maneuvers to ensure that the product of the probability of failure and the risk of human casualty during reentry shall not exceed 1:10,000 (NASA Requirement 56628.)

## 4. CONCEPT OF OPERATIONS

The *Curimba* mission employs a nanosatellite-carrying minisatellite, known as the mothership. After release from its launcher the mothership maneuvers into an orbit relative to the target debris and determines the attitude state of the target using on-board optical sensors and attitude determination algorithms [14], [15], [16], [17]. The relative attitude and position states are used to plan, on-board the mothership, the rendezvous and docking trajectories for each of the nanosatellites [18], [19], [20], [21]. Four of the six nanosatellites of the 12U class, (24 kg in mass and 240×240×360 mm in size), are sequentially deployed from the mothership, as illustrated in Figure 2.

Each nanosatellite uses its attitude and orbit determination sensors and miniaturized propulsion system to follow its pre-planned trajectory. Updates from its own sensors and from the mothership, with which it is in radio contact, allow the nanosatellite to re-plan the trajectory to take into account any changes in the state of the target and in the environment. Once in physical contact with the target, the nanosatellite latches on using an electrostatic adhesion mechanism [22], [23], [24], [25]. Once docked, the nanosatellites form a wireless network of distributed sensors and cooperate to further refine knowledge of the attitude state of the target, estimate the amount of residual propellant left in the tanks of the target, and assess its structural integrity. The results of the structural analysis are used to plan safe maneuver profiles for detumbling and deorbiting the target.

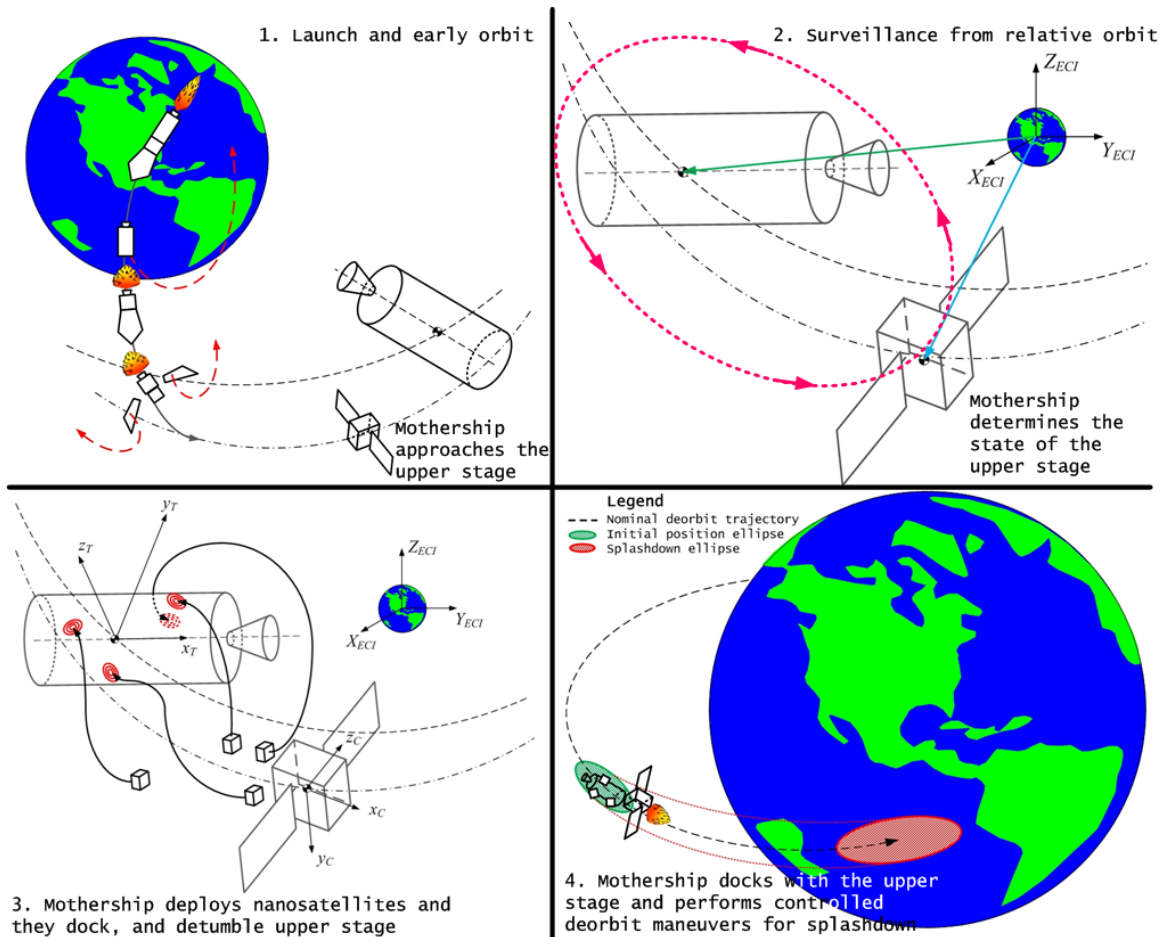


**Figure 2.** Storyboard for the concept of operations of the *Curimba* mission

The nanosatellites cooperatively use their thrusters to detumble the target and control its attitude. After the target is detumbled the mothership docks with it and performs reentry maneuvers aiming for a splashdown in an oceanic body of water. For the proof of concept proposed here, the mothership and nanosatellites remain latched to the target during reentry. A few alternative mission architectures are envisioned for follow-on missions. One architecture employs a set of a few specialized deorbit nanosatellites which dock with the already stabilized target and perform the reentry maneuvers. A more advanced architecture for the deorbit of multiple targets is also envisioned. After the detumble of the current target the nanosatellites that detumbled it separate and dock with the mothership to be refueled and carried to the next target.

#### *Active Debris Removal Target Selection*

The large debris objects considered for deorbit are uncontrolled satellites and RBs with a radar cross section (RCS) larger than  $5 \text{ m}^2$ . RBs are designed to withstand space launch loads so it is likely that they are sufficiently robust to maintain structural integrity during ADR docking and deorbit maneuvers. Uncontrolled satellites are a more challenging target than RBs due to various deployed appendages which have a limited capability to withstand structural loading and whose mounting points to the satellite bus have been exposed to the space environment for decades. The proposed mission concept is applicable to any large uncontrolled resident space object (RSO) in LEO. However, due to the practicalities of mission assurance and ADR concept demonstration, the targets selected for removal are RBs with an RCS larger than

$5 \text{ m}^2$ . Data retrieved from [Space-Track.org](http://Space-Track.org) on 31 Mar 2013 shows that Russia is the largest debris producer in LEO with a total of 487 RBs and the US is following far behind with a total of 153. The abundance of Russian RBs leads to the conclusion that they are a natural choice for an ADR mission. To this effect, both Liou [5] and Ryzhova [26] point to the second stage of the Kocmoc-1/3 launcher (US designation SL-8) as a likely candidate for an ADR mission. SL-8 has a diameter of 2.4 m, a length of 4.3 m and a dry mass of 1,440 kg. Despite the abundance of SL-8 stages and Ryzhova's [26] proposing an international collaboration for the ADR of an SL-8 stage the legal, political, and national security implications for the potential participants in an international ADR effort add multiple risks to an already complex mission. Therefore it is proposed that the ADR target is a United States (US) owned RB of similar size and shape to the SL-8. A study of the US owned RBs in LEO reveals that the venerable Agena D [27] with a diameter of 1.5 m, a length of 6.5 m, and a dry mass of 673 kg is a good match. The candidate targets for the ADR mission are selected by analyzing the distributions of orbital inclinations and RCS of the SL-8 and Agena D RBs, presented in Figure 3.

A good Agena D candidate for an ADR mission has an orbital inclination and RCS close to those of a large number of SL-8 RBs. Analysis of the distributions in Figure 3 shows that four Agena D RBs, with orbital inclinations of  $70^\circ$ , are within  $4^\circ$  of the orbital planes of 118 SL-8 RBs. Their orbital parameters are shown in Table 1 together with those of a representative SL-8 RB. For the purpose of the preliminary design work the Agena D with the largest cross-section, the

**Table 1. Orbital parameters of Agena D RBs and a representative Kocmoc 3/SL-8 RB**

Name	Intl. designation	NORAD designation	Launch date	Incl. (°)	Apogee (km)	Perigee (km)	RCS (m <sup>2</sup> )
Agena D	1964-001A	00727	11 Jan 1964	69.91	1078	906	4.866
	1965-016J	01245	9 Mar 1965	70.08	912	898	5.212
	1967-053B	02825	31 May 1967	69.97	923	888	6.644
	1969-082AB	04159	30 Sep 1969	69.96	919	902	7.469
SL-8	1972-009B	05847	25 Feb 1972	74.05	989	945	4.837

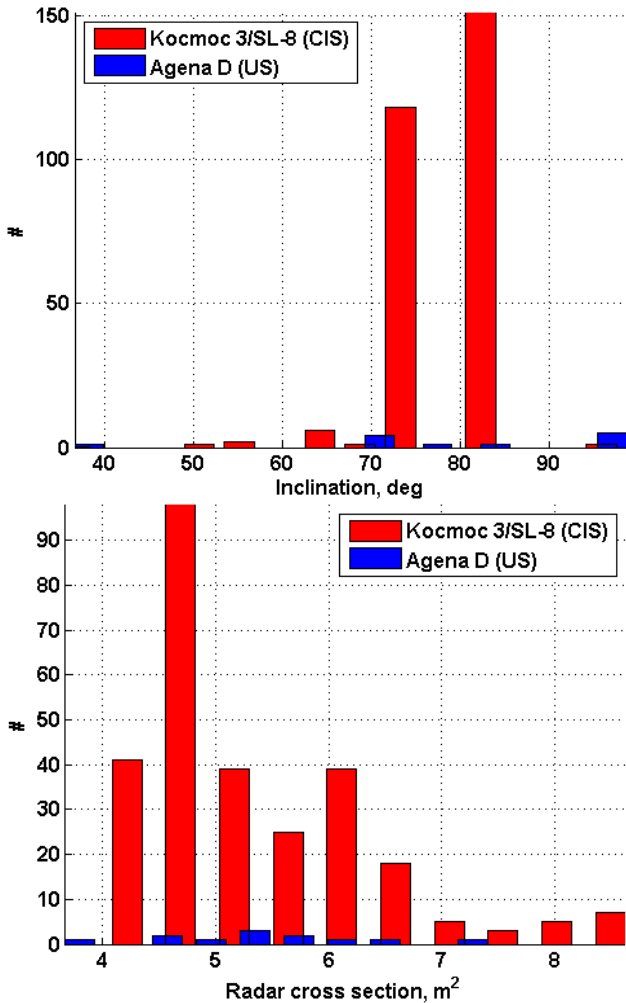


**Figure 3.** Distribution of inclinations (top) and radar cross-sections (bottom) of Kocmoc 3/SL-8 and Agena D RBs

1969-082AB/04159, is selected for study.

*Advantages and Credibility of the Proposed Concept*

The proposed concept revolutionizes the state of the art of ADR missions by employing a network of agile cooperating spacecraft that produces results beyond the capabilities of a complex monolithic satellite. *Curimba* brings together the practical aspects of rendezvous, proximity operations, docking, and spacecraft autonomy within the elegant framework of evolving systems [28], [29], [30], [31] and thus it provides a leap in the capabilities of multi-spacecraft missions.

Since it employs multiple nanosatellites, including spares, the

mission is robust to single point failure. The inherent scalability and flexibility of the networked system described here can be applied to future space missions such as 1) on-orbit servicing; 2) offensive and defensive space control; 3) human space flight for ISS surveillance and repair; and 4) deep space science missions for small body exploration. *Curimba* relies on well understood technologies of mid technology readiness levels (TRLs) employed in unique and novel ways to achieve complex tasks. A precursor nanosatellite of the 6U CubeSat class, the ARAPAIMA<sup>3</sup>, is currently designed under the supervision of the authors for the Air Force Office of Scientific Research (AFOSR) University Nanosatellite Program (UNP) Phase 8. ARAPAIMA has passed the UNP Engineering Design Review at the start of Aug 2014 and has been accepted in NASA's CubeSat Launch Initiative (CSLI). The majority of the nanosatellite subsystems and all the proximity operations algorithms developed for the UNP project are directly applicable to *Curimba*. By the start of a *Curimba*-like ADR mission the technologies will have been extensively tested in orbit. The only technologies with a low TRL are the docking algorithms and the docking mechanism, which rely on already demonstrated principles but have to be redesigned and adapted for an ADR mission. The parameter estimation for identification of the remaining propellant in the RB and of its structural integrity are relatively well understood [32], [33] and they will be extensively tested through numerical simulations and laboratory experiments. The mothership is based on a minisatellite bus with space heritage such as Orbital Sciences LEOStar-2 [34], Ball Aerospace BCP [35], and NASA Ames Modular Common Bus [36] families and thus presents a relatively low development risk. The only new hardware development for the mothership is the active docking mechanism.

Elements of the full mission can be tested in a phased approach. In Phase I two nanosatellites, similar to those of the full mission, are deployed together in LEO and are tasked to either dock with the upper stage that releases them or maneuver to the proximity of a large RB, dock with it and perform an extensive set of attitude maneuvers on it. Phase II has at least four nanosatellites, also deployed together and tasked to fully detumble an RB and validate the technologies to bring them to a TRL of 9. Phase III is a full mission with a mothership and six nanosatellites. The authors are quite enthusiastic about the concept because Phases I and II are in the realm of feasibility for a small business and a university team that collaborate under the aegis of a government organization that facilitates the policy and programmatic hurdles of access to either the launch vehicle upper stage or to an RB. Phase I could be descoped at the discretion of the government program office, to save cost and schedule, and be replaced with comprehensive testing on parabolic flights and on the

<sup>3</sup>www.eraucubesat.org

ISS. The proposing team is also well aware of the legal, regulatory, and strategic challenges of ADR missions [37]. The phased approach of the *Curimba* mission is planned to reduce the risk and cost of ADR missions and thus lower the acceptance threshold by eventual customers.

An ADR mission such as *Curimba* is in direct accordance with the National Space Policy of the United States of America [38], which directs all sectors of the space industry to “pursue research and development of technologies and techniques, through the Administrator of the National Aeronautics and Space Administration and the Secretary of Defense, to mitigate and remove on-orbit debris, reduce hazards, and increase understanding of the current and future debris environment.” Furthermore, in 2012 the Committee on the Peaceful Uses of Outer Space of the United Nations Office for Outer Space Affairs published a report [37] in which it declares that “active removal of space debris and on-orbit satellite servicing should be undertaken by all stakeholders as soon as possible.”

## 5. FEASIBILITY ANALYSIS

NASA's Debris Assessment Software (DAS) has been used to perform the survivability analysis of the Agena D RB (1969-082AB/04159) during reentry. Of the 64 components included in the DAS model only the propellant tank and the engine survive reentry. The resulting casualty area and kinetic energy at impact for the propellant tank are 10.15 m<sup>2</sup> and 25.9 kJ, and for the engine are 5.82 m<sup>2</sup> and 53.7 kJ respectively. The population density on the ground track of the 70° inclination orbit of the target is on average 15 persons/km<sup>2</sup>. In the event of a land impact the resulting casualty risk from an uncontrolled reentry is 1.52:10,000 for the propellant tank and 0.87:10,000 for the engine and thus, the acceptable probabilities of failure are 65.7% and 100% respectively [39]. Consequently, the Agena D RB (1969-082AB/04159) will be deorbited with a controlled reentry that targets a safe zone in the Pacific.

The first step of the preliminary mission design have been undertaken to derive systems engineering budgets. Astrogator, the maneuver design tool of the AGI System Tool Kit (STK) has been used to design the phases of the mission which include the maneuvers of the mothership from release from its launcher to a relative orbit of 5 km radius about the RSO. The trajectories of the nanosats launched sequentially from the same point on the relative orbit 5 km behind the target have been designed and the results of optimal propellant maneuvers are discussed. The worst case scenario detumbling of the target by the nanosats has also been analyzed and the propellant required has been added to their propellant budget. Last but not least, a Monte Carlo analysis of the reentry has been performed to determine preliminary requirements for the pointing accuracy of the deorbit maneuver and the size of the splashdown ellipse. The results of the preliminary mission design are discussed in the following sections.

### *Mothership Preliminary Design*

The design of the mothership is centered around a demilitarized Peacekeeper post-boost propulsion subsystem (RS-34) and is somewhat inspired by the work presented by Esther et al. [40]. A rendering of the mothership is shown in Figure 4 and the functional diagram is presented in Figure 5. The mothership is a three-axis stabilized spacecraft that comprises a bus and a small ESPA ring [41], [42]. It has been designed

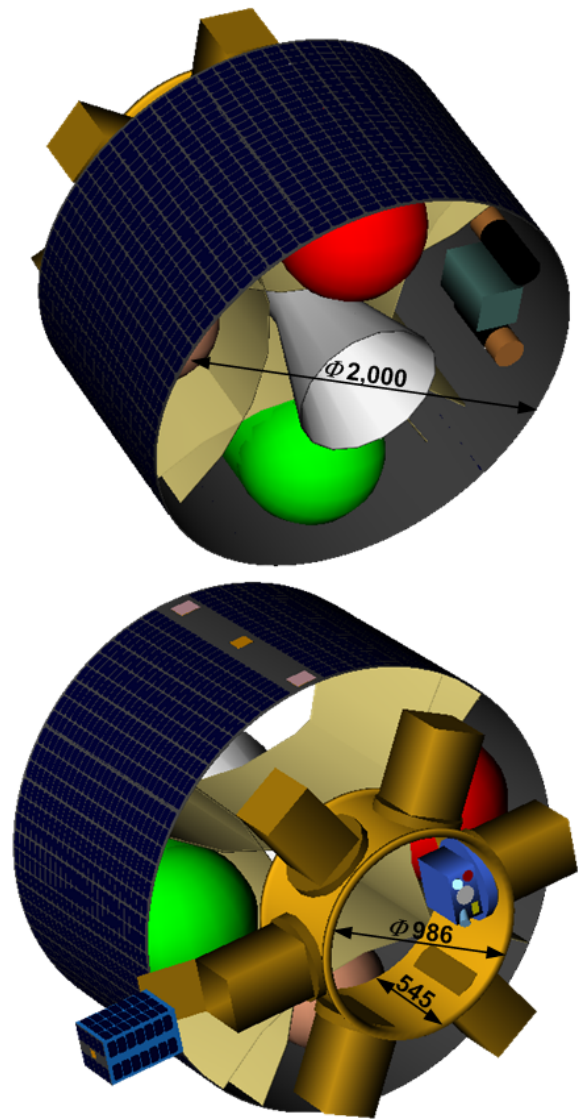


**Figure 4.** Renderings of the *Curimba* mothership with six CSDs. All dimensions are in mm.

to fit in a volume of 2,057 mm diameter and 1,948 mm height inside the Model 92 payload fairing of a Lockheed Martin Athena IIc launcher [43], [44]. The small ESPA ring fits the Model 38 payload adapter of the Athena IIc.

The mothership bus provides electrical power, telecommunications, attitude determination and control, orbit determination and control functions, relative navigation, and on-board computing and commanding. The solar power subsystem employs body mounted solar cells that charge batteries and provide power to the subsystems via a power regulation and distribution module. The telecommunication subsystem consists of a ground station transponder that uses S-band for both uplink and downlink. The inter-spacecraft communications architecture, shown in Figure 6, is based on the L-3 Communications Net-T [45] architecture which implements an IP-based full duplex secure system with a hub and spoke topology.

Net-T has heritage from tactical military applications and it is self-scaling, i.e., communication nodes come in as they become available and go out as they lose contact, and auto-optimizing, i.e. the uplink bandwidth is optimized to reduce

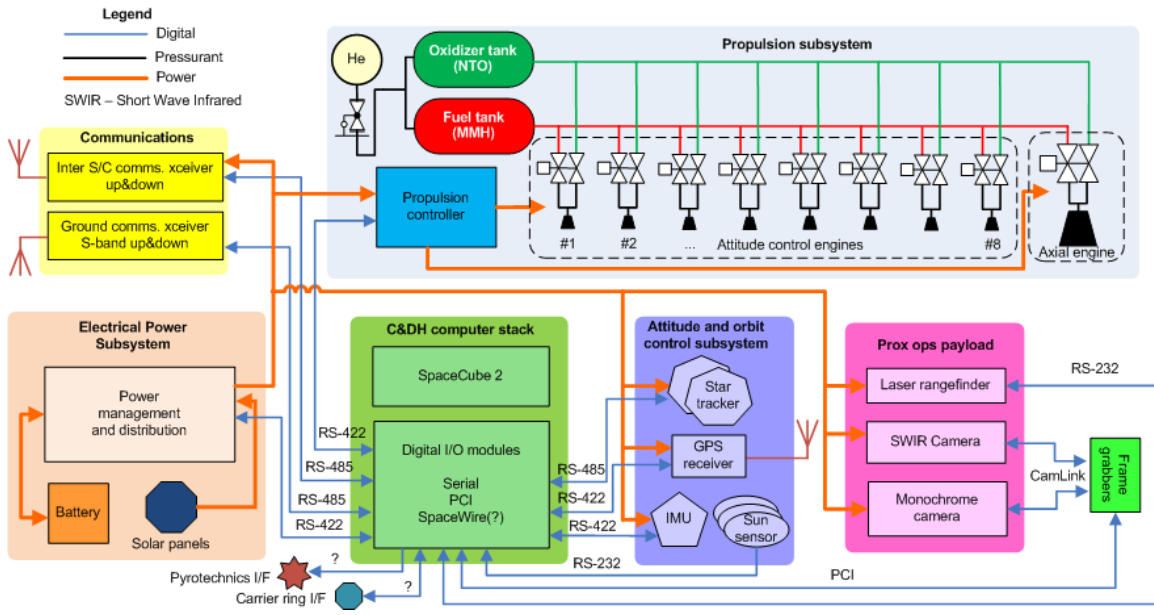


**Figure 5.** Functional diagram of the *Curimba* mothership. Fill and relief valves, filters, and propulsion subsystem pyrotechnics are not shown.

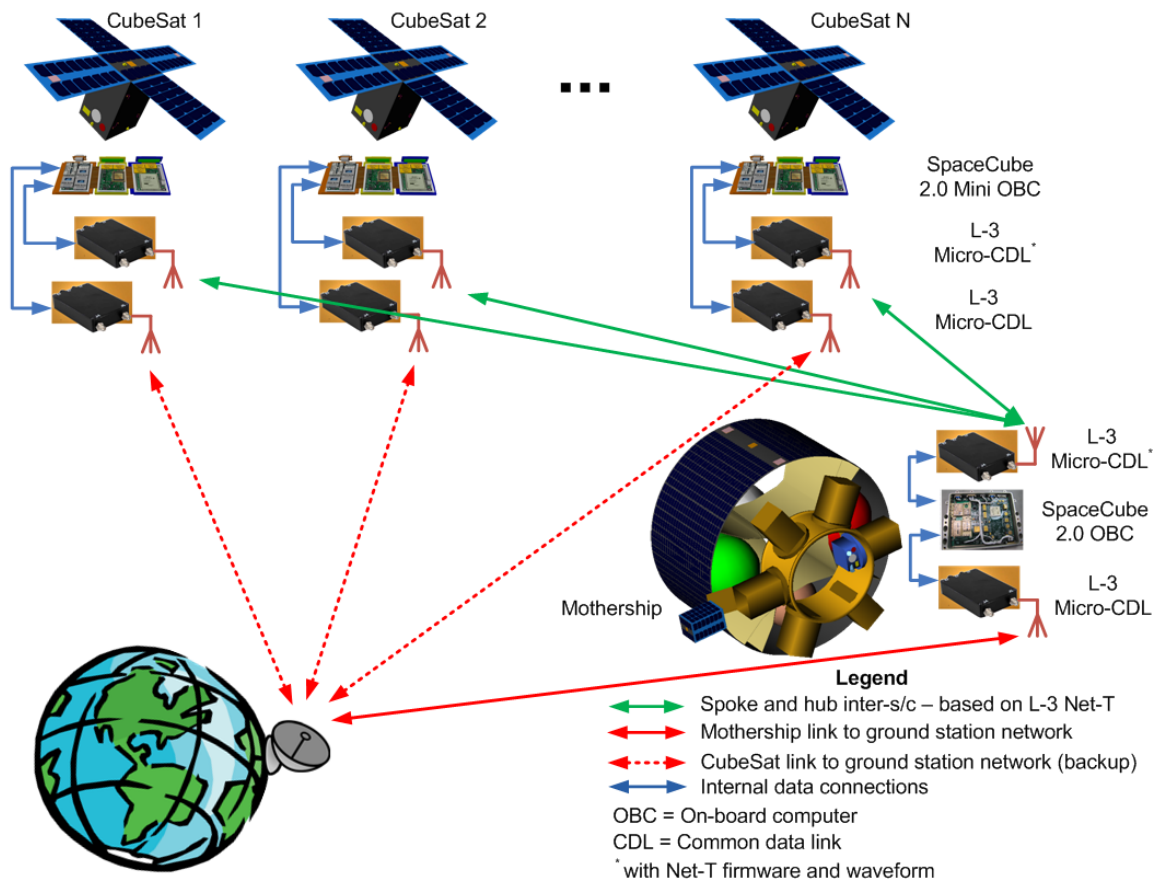


**Figure 6.** Diagram of the *Curimba* communications architecture

**Table 2. Mass budget for the Curimba mission**

Name	Unit mass (kg)	#	Mass (kg)
12U CSD	6.02	6	36.12
Ring	100.00	1	100.00
Avionics+pwr	50.00	1	50.00
Mothership (dry)	366.67	1	366.67
Dry mass			552.79
Contingency	25%	1	138.20
Dry mass w/ contingency			690.98
12U CubeSat	24.00	6	144.00
Dry mass w/ CubeSats			834.98
Propellant	300.00	1	300.00
Total mass			1134.98
Athena IIc to 850 km & 70°			1160.00

packet collisions. The attitude determination subsystem consists of sun sensors for coarse attitude determination and an IMU that works together with a pair of star trackers for fine attitude determination. Attitude control is accomplished with eight attitude control engines (ACE). The selection of the size of the ACEs has been left for the second iteration of the mission design with the choice between 22 N [46] and 110 N [47] bi-propellant thrusters from Aerojet. Use of the original 312 N RS-34 ACEs[40] has also been considered. However, the lack of data on their minimum impulse bit and other operational parameters had given them the lowest ranking in the options list for the attitude control of the mothership. Orbit determination is provided by a GPS module and an on-board orbit propagator as backup. Orbit control is provided by the bi-propellant, nitrogen tetroxide (NTO) and monomethylhydrazine (MMH), axial engine (AXE) which produces 11.8 kN of thrust at a specific impulse of 308 s. The relative navigation functions are provided by a proximity operations payload that consists of a monochrome camera with an aperture of 90 mm, a short wave infrared (SWIR) camera with an aperture of 45 mm, and a laser rangefinder (LRF) with a range of 10 km. The mothership on-board computing and data handling (C&DH) is accomplished with a SpaceCube 2.0 [48], [49] computer designed by the NASA Goddard Science Data Processing Branch. The overall size of the mothership bus is 2,000 mm in diameter and 1,200 mm in height. For the purpose of the first iteration of the mission design it has been assumed that the mass of the bus is equal to that of the Peacekeeper RS-34 post-boost stage which is conservative, because the RS-34 has been designed to withstand the rigors of an ICBM transport and eventual launch. The small ESPA ring from Moog [41], [42] can carry up to six 12U canisterized satellite dispensers (CSD) [50]. The ring has a height of 545 mm and a diameter of 986 mm. The CSDs are installed radially on the exterior of the ring so that the CubeSats are ejected radially outwards. The mass budget for the mothership is presented in Table 2. The budget includes a system-level contingency of 25%, applied to the dry mass of the mothership. An Athena IIc launched from the Kodiak, Alaska, launch complex can orbit a payload of 1160 kg in a circular orbit of 850 km and 70° inclination [43]. In conclusion, the mission can be launched by the Athena IIc, albeit with a narrow margin of 15kg.

#### CubeSat Preliminary Design

The 12U CubeSat is a three-axis stabilized spacecraft of 240×240×360 mm and a mass of 24 kg. Its rendering is

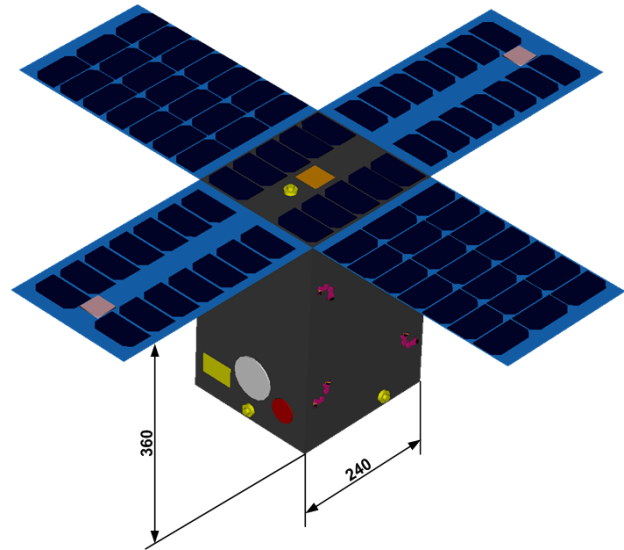


**Figure 7.** Rendering of the *Curimba* 12U CubeSat with solar panels deployed. All dimensions are in mm.

presented in Figure 7 and its functional diagram in Figure 8.

The CubeSat has a full complement of subsystems: power, propulsion, attitude determination and control (ADCS), orbit determination, and computing and commanding. Its optical payload consists of the same instruments as the proximity operations payload of the mothership and it is planned that their designs are approximately 90% common. From a mechanical point of view the most important difference is the placement of the star tracker on the CubeSat so it points opposite from the proximity operations payload. The active electrostatic docking mechanism, illustrated in Figure 9, is considered part of the payload. It has its own controller to adjust the curvature and the electrostatic adhesion force and it is operated in closed loop with the CubeSat ADCS. The propulsion system of the CubeSat is a miniaturized system consisting of 16 solenoid-fed thrusters placed such that they generate positive and negative torques about all three body axes with dual redundancy. The thruster arrangement also generates positive and negative forces about two of the three body axes. The propellant is 1,1-difluoroethane [51], which can generate about 70 s of specific impulse. For the first design iteration it has been assumed that each thruster produces 50 mN. The CubeSat C&DH is accomplished with a SpaceCube 2.0 MINI [52] also designed by NASA's Goddard Science Data Processing Branch. Besides the size, the major difference between the mothership and CubeSat on-board computer configurations is that the mothership uses the Virtex-5QV FX130 S1RF radiation hardened parts and the CubeSat uses the commercial Virtex 5 FX130T. The telecommunications subsystem of the CubeSat is identical with that of the mothership. Four deployable solar panels and one fixed panel provide electrical power to the power conditioning and distribution unit. A battery of at least 100Wh capacity completes the power subsystem.

## 6. MANEUVER DESIGN AND PLANNING

This section presents the preliminary design and analysis of the maneuvers of the mothership and of the CubeSats. AGI's Astrogator tool has been used to perform the maneuver design for the mothership. The CubeSat maneuvers have been planned with a minmax optimizer applied to the linear equations of motion [53]. Both the mothership and CubeSat

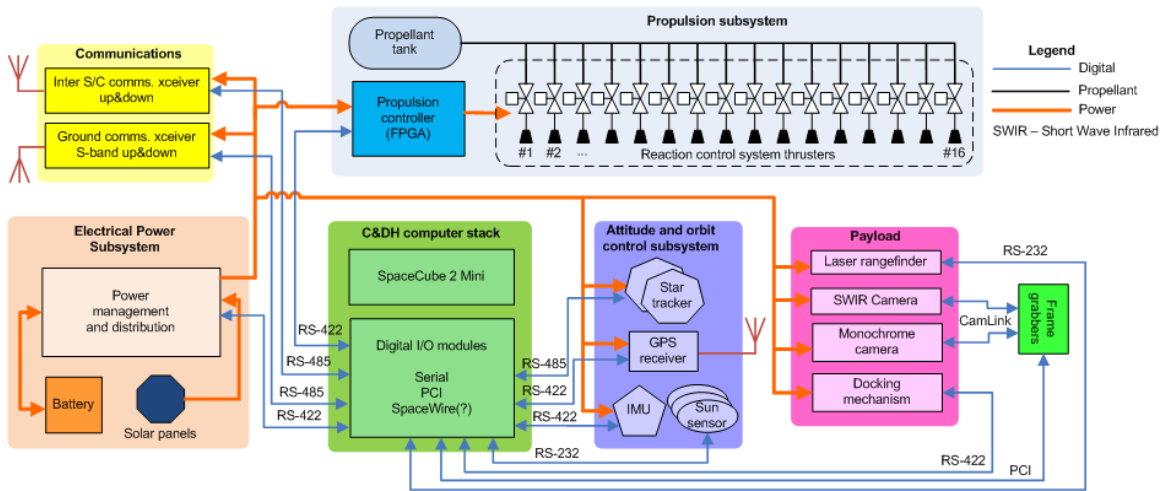


Figure 8. Functional diagram of the Curimba 12U CubeSat

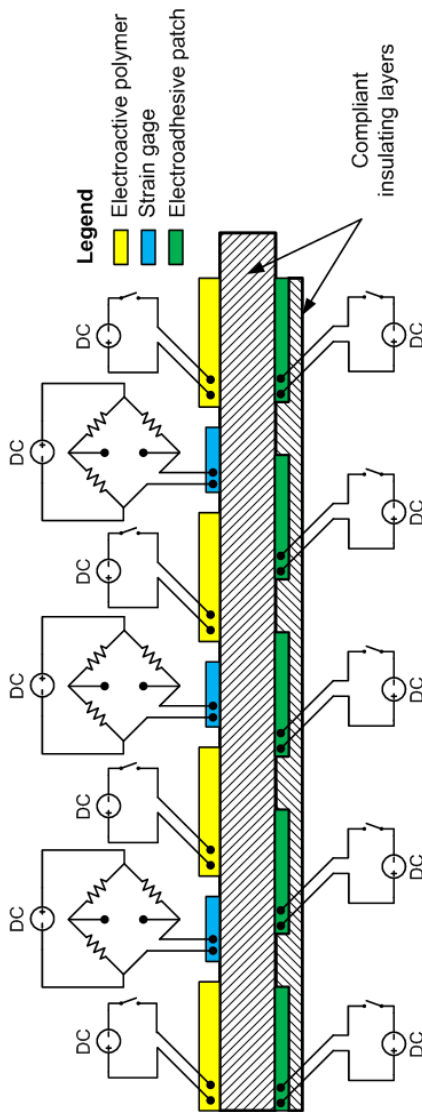
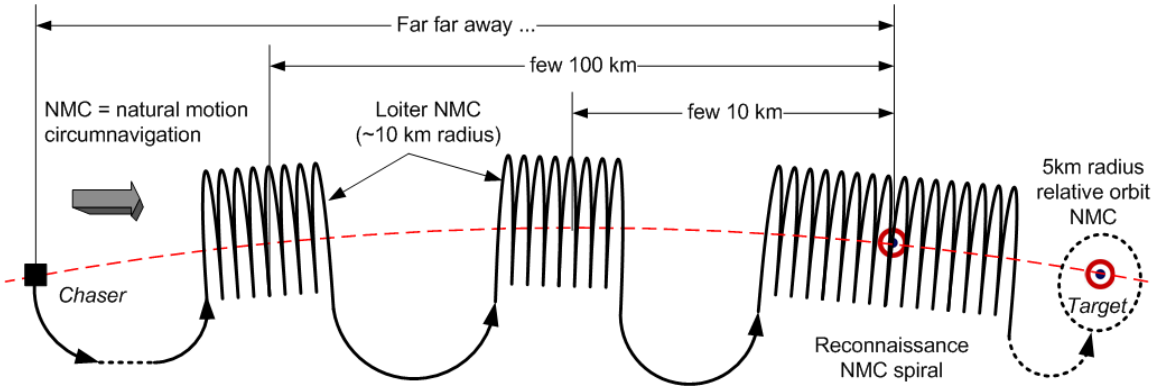


Figure 9. Schematic of the active electrostatic adhesive docking mechanism. The electroactive polymer patches change the curvature of the mechanism.

trajectories have been propagated with the high precision orbit propagator of Astrogator HPOPv1.0.

#### Mothership Rendezvous and Proximity Operations

A notional launch date of 1 Jan 2016 has been chosen. It has been assumed that the mothership is released in a circular orbit of 850 km altitude such that it is phased at  $-180^\circ$ , i.e., it is at a diametrically opposite point in the orbit from the target and following it. The plan for the early orbit operations is to perform a systems shakedown and calibration in the first week from release. A stepwise maneuvering plan is designed so that the mothership approaches the target from the start of early orbit operations. The goal of the maneuvers is to bring the mothership into a circular relative orbit of 5 km centered at the target. An illustration of the approach is schematically shown in Figure 10. The propellant use for the rendezvous and proximity maneuvers with the target have been designed with Astrogator. The trajectories of the mothership with respect to the target are presented in Figure 11 and the results are discussed below. The first maneuver is a typical two-burn Hohmann phasing maneuver which places the mothership 250 km behind the target. The following maneuvers are designed to place the mothership in a so called loiter natural motion circumnavigation (NMC) in which the spacecraft moves in a relative orbit with respect to a point at a certain distance from the target. Two loiter NMCs are planned, both circular and with a radius of 15 km. The first loiter NMC is centered at 35 km and the second at 6 km behind the target. The second NMC is designed such that, at the closest point, the mothership approaches the target within its LRF range, 10 km, and can validate the outcome of the maneuver. In terms of relative motion, the mothership transitions between the two loiter NMCs on a spiral NMC. Prior to acquiring a relative orbit centered at the target the mothership performs an observability maneuver which initiates an NMC in a plane approximately perpendicular to that of the previous loiter NMC. Angles only measurements of the target taken during the observability NMC decrease the uncertainty of the relative navigation solutions of the angles-only relative navigation (AoN) algorithms. For the preliminary design presented here it has been assumed that the mothership autonomously performs relative orbit maintenance maneuvers once per orbit. The results of the relative orbit maintenance maneuver design show that the large AXE (11.8 kN) has to fire for 6 ms which is unrealistic. If the AXE cannot satisfy the MIB requirement then the ACEs will be used to perform



**Figure 10.** Schematic of the approach to target

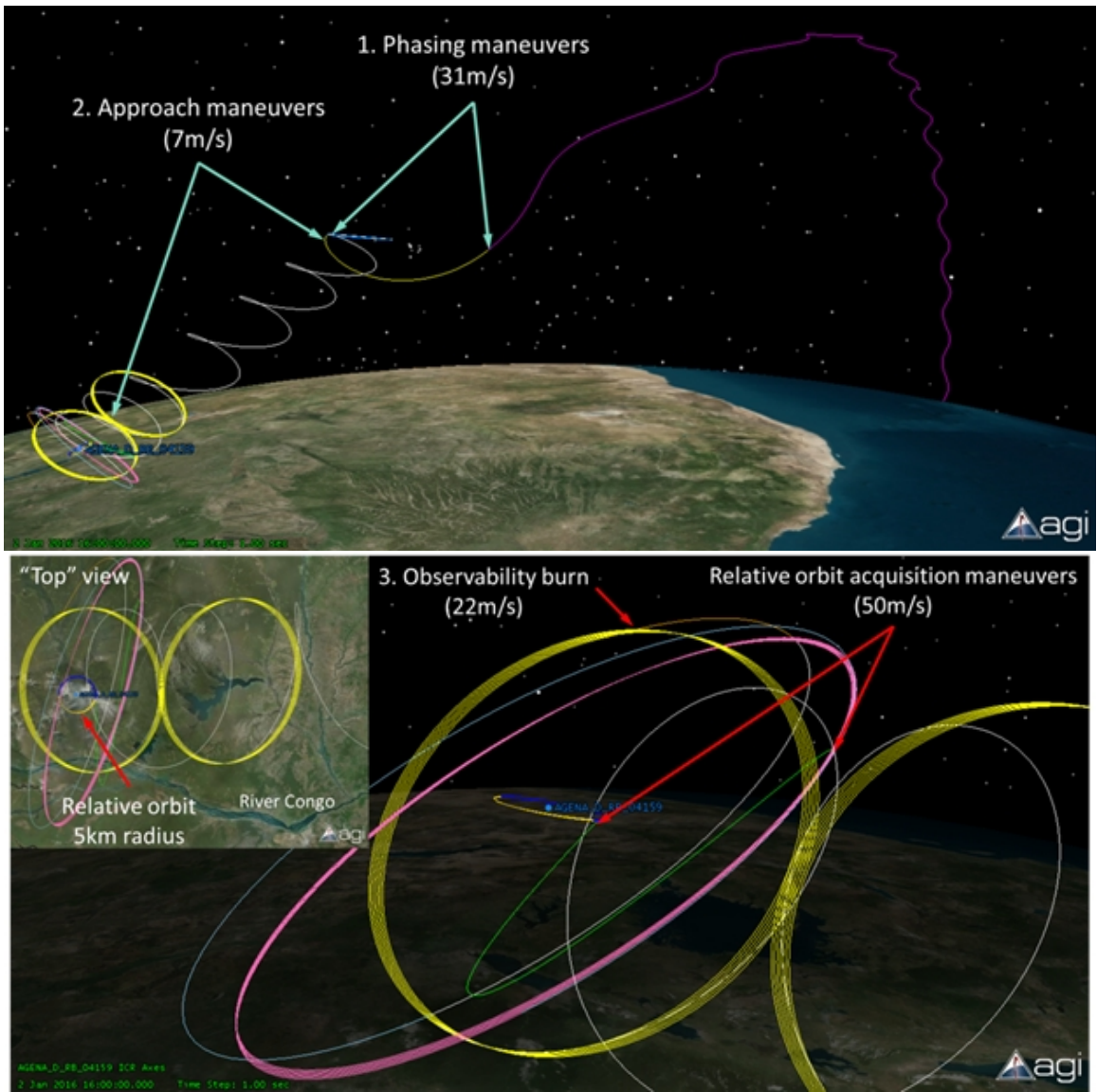


**Figure 11.** Target relative trajectories of the mothership with respect to the Agena D target. Full view (top) and zoom in (bottom) of the loiter NMC and relative orbits.

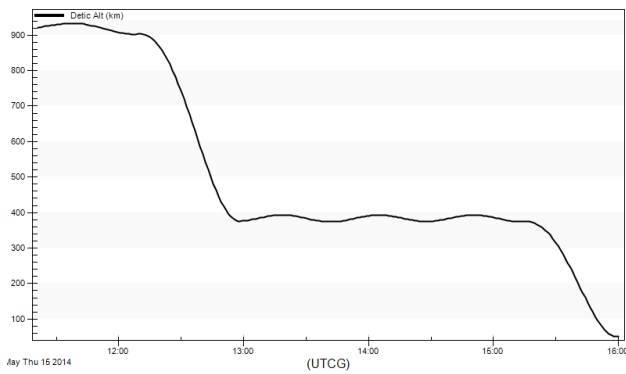


**Figure 12.** Altitude vs time for the deorbit phase of the mission

the relative orbit maintenance maneuvers.

### Reentry Maneuver Design

The reentry maneuver is planned in a manner similar to that described by Craychee [54], which was successfully employed to deorbit the OrbView-3 commercial Earth observation satellite in 2011. The deorbit maneuvers are performed by the mothership which is assumed to be docked with the target. The CubeSats are assumed to be latched to the target and reenter with it. If further design iterations determine that the deceleration forces applied during the deorbit maneuver overcome the docking mechanism hold-down capability, the CubeSats will detach after the mothership docks with the target and they will perform reentry on their own.

The deorbit maneuvers are designed to reduce the time in an orbit crossing the ISS orbit, similarly to those of [54]. The deorbit commences with two Hohmann maneuvers which place the mothership-target-CubeSats stack in a parking orbit. The parking orbit is circular with an altitude of 375 km which is 50 km lower than ISS orbit at the time of this writing. After three revolutions in the parking orbit the mothership maneuvers to achieve a perigee of 50 km, which is considered a targeted reentry in NASA procedures [39]. The evolution of the altitude vs time is presented in Figure 12.

A safe splashdown zone has been designated in the Pacific with boundaries at least 1000 km from any landmass, similar to [54]. A Monte-Carlo analysis has been performed with STK Astrogator and STK Analyzer to determine the pointing and orbit determination requirements at reentry burn. It has been assumed that at the time of the reentry maneuver the pointing accuracy is of  $0.1^\circ$  half cone ( $3\sigma$ ) and the burn time accuracy is of 1 s ( $3\sigma$ ). Both uncertainties follow a Gaussian distribution. A wind gust with a speed between -30 m/s and 30 m/s in a direction normal to the plane of the trajectory has been applied at 50 km with a uniform distribution. The results of 1000 Monte Carlo simulations, integrated all the way down to sea level, and presented in Figure 13, show that the splashdown ellipse has axes of 120 km by 10 km and fits well inside the safe zone.

Current work focuses on improving the fidelity of the wind model for the duration of the reentry trajectory by including the horizontal wind mode (HWM<sup>4</sup>) and eventually the Earth Global Reference Atmospheric Model (GRAM 2010<sup>5</sup>).

<sup>4</sup><http://ccmc.gsfc.nasa.gov/modelweb/atmos/hwm.html>

<sup>5</sup>[http://see.msfc.nasa.gov/tte/model\\_gram.html](http://see.msfc.nasa.gov/tte/model_gram.html)

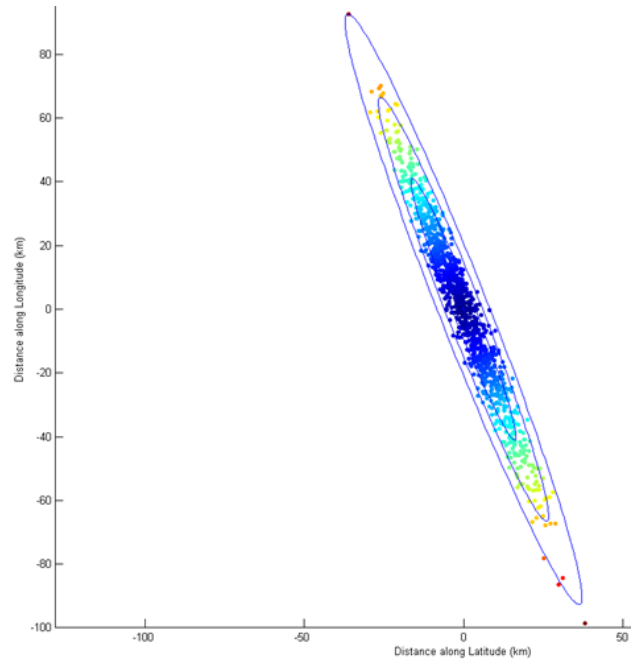


**Figure 13.** Dispersion of the splashdown locations at sea level. Ellipses are the 1,2, and 3  $\sigma$  bounds.

### Mothership Propellant Budget

The results of the rendezvous and proximity operations maneuver designs for the mothership are presented in Table 3. The results of the deorbit maneuvers are presented in Table 4. It is assumed that mothership applies a total of 100 relative orbit maintenance maneuvers, each of  $\Delta V = 0.065$  m/s. Assuming that they are applied every other orbit the overall duration of relative orbiting with respect to the target is about two weeks. The propellant use for the entire mission is shown in Table 5. The total  $\Delta V$  required, without including any contingencies is 517 m/s which is well below the 927 m/s available in the propellant tanks of the mothership.

As a consequence, more than 35% of the full propellant load is left in the tanks of the mothership at the completion of the targeted reentry maneuver. Assuming a 25% contingency, sufficient propellant is left in the mothership to raise its orbit and perform space based situational maneuvers or technology experiments. It should be noted that the maneuvers described here have not been optimized for minimum propellant and it is expected that refinement of the observability and relative orbit acquisition maneuvers could save up to 10% of the propellant used by the current maneuvers. Smaller but significant propellant savings can be achieved during the reentry by performing small orbit lowering maneuvers and letting the atmospheric drag naturally decay the orbit between maneuvers.

### CubeSat Maneuver Design

It has been assumed that each CubeSat is ejected from the mothership from the same point of its relative orbit of 5 km radius and that it starts maneuvering on its own at a range of about 1 km from the target. The dynamic model of the relative motion is given by the Hill-Clohesy-Wilshire (HCW) equations [53] and a minmax propellant optimal problem has been set up similarly to that described by Tillerson [55], [56]. The goal of the propellant optimal maneuvers is to achieve null relative velocity at a distance at the target in two orbits, approximately 220 min. The results of the optimal maneuvers

**Table 3. Mothership propellant use for the rendezvous and proximity operations maneuvers**

Segment name	$\Delta V$ (m/s)
Phasing #1	15.57
Phasing #2	15.37
Phasing tot.	30.95
Start approach # 1	2.60
Stop approach # 1	2.60
Start approach # 2	1.04
Stop approach # 2	1.04
Approach tot.	7.28
Observability burn	21.78
Stop observability drift	0.26
Observability tot.	22.04
Prepare rel. orbit acq.	29.51
Relative orbit acquisition	20.51
Relative orbit tot.	50.02
Total	110.29

**Table 4. Mothership propellant use for the deorbit maneuvers**

Segment name	$\Delta V$ (m/s)
Hohmann to park #1	144.86
Hohmann to park #2	145.22
Park to splash	95.41
Total	385.50

thus obtained have been used in STK Astrogator to analyze the trajectory in the presence of perturbations. Astrogator's high precision orbit propagator (HPOPv10) which includes a high accuracy geo-potential model, drag, and third body effects, has been used to simulate the relative motion between the CubeSat and the target. As expected, the end state of the trajectory is no longer the one obtained from the linear optimization problem. Perturbations to the motion of the CubeSat make it depart from the optimal trajectory and the end state is 20 m from the target with some small but finite relative speed. Thus, the CubeSat slowly drifts away from the target reaching approximately 100 m from it in five orbits. Figure 14 shows the trajectory of one CubeSat relative to the target.

Ongoing research focuses [21] on the investigation of optimal trajectories in the presence of perturbations, namely from Earth oblateness ( $J_2$ ) and drag. The trajectories can then be used to generate translational and rotation maneuver commands for CubeSats [57].

For the time being the CubeSat proximity operations have not been designed and analyzed. However, it is planned that once within a few km from the target the CubeSat uses its own relative navigation sensors and algorithms in order to close the loop and achieve a perching state above a point of interest on the target. From the perching point it "descends" to touch-

**Table 5. Mothership overall propellant use**

Segment name	$\Delta V$ (m/s)
Early orbit	38.23
Prox. ops. w/out maint.	86.63
Rel. orb. maint. $\times 100$	6.54
Deorbit	385.50
Grand total	516.89
Available	927.00

**Table 6. CubeSat propellant use**

Segment name	$\Delta V$ (m/s)
CubeSat detumble	0.06
Transfer (MS to RB)	0.90
Docking ops	0.90
Target detumble	0.25
Target analys.	0.30
Total	2.41
System cont. (200%)	4.82
Total w/ cont.	7.23
Available	35.00

down on the target and latches on to it. Once all six CubeSats are latched on the target they perform a distributed parameter system identification on the target to refine its attitude state and determine safe detumble and deorbit maneuver profiles.

Detumbling of target is performed cooperatively by the CubeSats latched to it. Assuming a uniform mass distribution the moment of inertia of the target Agena D RB has been estimated to be [2112.3, 2128.6, 166.8] kgm<sup>2</sup>. A worst case scenario for the angular rate of the RB has been considered, with 20°/s about each body axis.

The results of the CubeSat maneuvers described in this section are summarized in the propellant budget Table 6. Each of the entries above the total row in the table include 200% contingency to account for uncertainties. Since the CubeSat propulsion system carries a total  $\Delta V$  of 35 m/s at a first look it might seem that it is overdesigned, because it holds almost five times the required propellant. A better point of view is to think that due to the additional propellant the CubeSat has at least five chances to attempt latching with the target if it is unsuccessful in the first attempt.

## 7. CONCLUSIONS

A preliminary maneuver design has been performed to demonstrate the feasibility of an ADR mission with a multi-satellite mission comprising a mothership and six nanosatellites of the 12U CubeSat class. The results are encouraging and show that sufficient propellant margins are available in the current design. A second iteration of the design will be undertaken to prepare for a Mission Concept Review before the end of 2014. The major challenges identified during the preliminary design are presented together with ways of

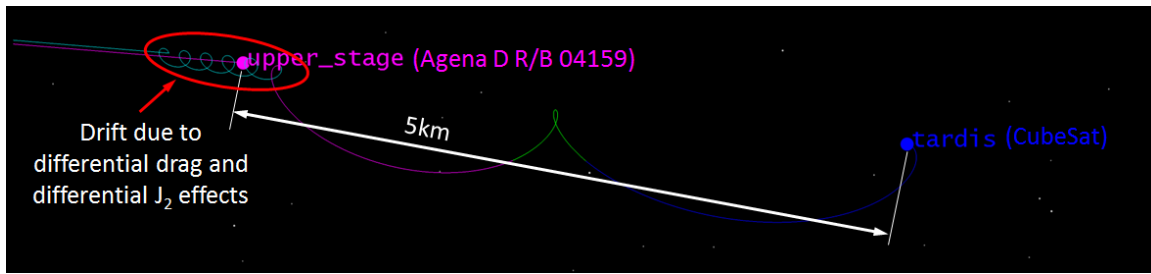


**Figure 14.** Propellant optimal relative trajectory of the CubeSat with respect to the target.

addressing them in the immediate future in the appendices.

For the design iteration presented here it has been assumed that the mothership carries the full complement of six 12U CubeSats and a full, 300 kg, propellant load. The goal of a second design iteration is to investigate the capability of the mission to detumble one RB with only three CubeSats, and then deorbit it. The other three CubeSats and the propellant leftover in the mothership will be used to detumble a second RB and either deorbit it or raise its orbit so that it poses negligible collision risks.

## APPENDICES

### A. BENEFITS OF THE MISSION STUDY

From a technical point of view the most important benefits of the study come from determining the feasibility of the mission, determining low TRL technologies that will have to be advanced to reduce mission risk, and establishing a mission baseline, which has been used to estimate costs. One of the benefits of the study might be the reduction of ADR mission costs below the billions of dollars predicted by Jakhu [37] and Wiedemann [58]. An indirect benefit of the work is the initial development of algorithms to support complex heterogeneous multi-satellite mission design. From the authors experience in formation flying mission design [59], [60], [61], [62], [63], [64], [65], [66], early algorithm development for cooperative multi-satellite missions has the advantage of their being adopted as powerful systems engineering tools that allow rapid trade studies and the analysis of what-if scenarios. Immediate societal benefits of the project come from engaging students to work on complex space mission designs and from incorporating highlights of the *Curimba* mission in STEM outreach at local schools. Intermediate contributions could arise from application of the evolving systems algorithms on projects in which independent systems, with individual feedback control, self-assemble to satisfy requirements unreachable by a single system, e.g., DARPA's Tactically Expandable Maritime Platform (TEMP) [67] and large orbiting power stations [68].

### B. UNDERSTANDING OF MAJOR CHALLENGES

The major technical challenges are mapped to corresponding study objectives and they are presented together with paths for risk reduction.

#### 1. Detumble operations

- The angular rate of the Agena D upper RB is unknown: research in the field of rotational states of RBs is active [69], [70], [71], [72], [73], [74]. So far, simulation results point

to angular rate magnitudes of maximum  $10^\circ/\text{s}$  per axis. This rate is assumed for initial simulations. NASA's Orbital Debris Program Office (ODPO) plans to validate the results of laboratory and numerical simulation studies with light curve data collected for potential ADR targets [75].

- The amount of propellant left in the RB propellant tanks and the RB structural integrity are unknown: at the time of this writing it is not clear if the Agena D RBs were passivated at the end of mission by venting the remaining propellant. In addition, long exposure to the space environment might have weakened the structure. Since the mission is designed with the ultimate goal of deorbiting targets that are not passivated and of varying ages and shapes, the estimation and control algorithms should be sufficiently robust to handle propellant slosh and structural uncertainties; they will be extensively validated through simulations.

#### 2. Initial algorithm development

- Algorithms for docking with the target: are employed from the moment the nanosatellite is a few centimeters away from the target to the moment it is securely latched to the target. The relative position and attitude control loops are closed with sensors installed on the electro-adhesive docking mechanism.

- Algorithms for the distributed parameter estimation of the leftover propellant and structural integrity: assuming, in a first approximation, linear models of the structural dynamics of the target allow the application of the methods developed by Kar et al. [76], [77], [78] for the determination of conditions for observability, sensing devices, and sensor connectedness. The conditions have direct applicability to determining mission systems budgets.

- Algorithms for the cooperative detumbling of the target: are developed organically with the estimation algorithms mentioned above. Adaptive control algorithms, which allow the nanosatellites to control a plant with highly uncertain dynamics and uncertain but bound disturbances, such as those presented by Nelson et al. [79] are implemented in the framework of evolving systems developed by Frost and Balas [80], [30]. The minimum number of nanosatellites required to detumble the RB is also determined at this stage.

#### 3. Reentry design and analysis

- Assessment of the demise of RB during reentry: is used to determine the size of the impact zone of any surviving debris and the casualty risk and to select the geographic location and altitude of a reentry perigee. The breakup altitude is, in general, assumed to lie between 75 and 85 km [81]. However, the Agena D RB considered here, has been exposed to the effects of highly energetic particles and thermal cycling in LEO for half a century and might breakup at higher altitudes. The deorbit maneuver planning should take into account this eventuality and determine the sensitivity of the shape and size of the impact zone to the breakup altitude.

## ACKNOWLEDGMENTS

Mr. Chris Mimms (VisSidus intern) for the optimal trajectory design for the CubeSat and the Monte Carlo analysis of the splashdown ellipse. Dr. J.C. Liou, NASA Chief Scientist for Orbital Debris for advice on orbital debris and spacecraft demise tools. Prof. Mark Balas from ERAU Aerospace Engineering for his advice and hand-holding on advanced topics in adaptive and robust control.

## REFERENCES

- [1] J.-C. Liou and D. Shoots, "Orbital debris quarterly news - vol. 16-2," 2012.
- [2] P. B. d. Selding, "Space station required no evasive maneuvers in 2013 despite growing debris threat," *Space News*, 2014.
- [3] J.-C. Liou and D. Shoots, "Orbital debris quarterly news - vol. 18-4," Lyndon B. Johnson Space Center, NASA, Tech. Rep., 2014.
- [4] DoD, *Department of Defense Instruction 3100.12*. Department of Defense, 2000.
- [5] J.-C. Liou, "An active debris removal parametric study for leo environment remediation," *Advances in Space Research*, vol. 47, no. 11, pp. 1865–1876, 2011.
- [6] M. H. Kaplan, "Survey of space debris reduction methods," in *2009 AIAA Space Conference and Exposition*, 2009.
- [7] B. Weeden, "Overview of active debris removal," in *2010 Beijing Orbital Debris Mitigation Workshop*. Secure World Foundation, 2010.
- [8] D. Alary, "Astrium's views on on-orbit servicing and active debris removal," in *2012 European On-Orbit Satellite Servicing and Active Debris Removal Conference*, 2012.
- [9] O. Colatis, D. Alary, R. D. Costa, and A. Pisseloup, "Airbus defence and space vision on active debris removal," in *3rd European Workshop on Space Debris Modelling and Remediation*, 2014.
- [10] M. M. Castronuovo, "Active space debris removal - a preliminary mission analysis and design," *Acta Astronautica*, vol. 69, no. 910, pp. 848–859, 2011.
- [11] N. Okada, "Active debris removal using carrier and multiple deorbiting kits," in *3rd European Workshop on Space Debris Modelling and Remediation*, 2014.
- [12] NASA, *Process for Limiting Orbital Debris (NASA-STD 8719.14)*. National Aeronautics and Space Administration, 2012.
- [13] C. Bonnal, J.-M. Ruault, and M.-C. Desjean, "Active debris removal: Recent progress and current trends," *Acta Astronautica*, vol. 85, pp. 51–60, 2013.
- [14] O. Yakimenko, V. Dobrokhodov, I. Kaminer, and R. Berlind, "Autonomous video scoring and dynamic attitude measurement," in *18th AIAA Aerodynamic Decelerator Systems Technology Conference and Seminar*, 2005.
- [15] F. Aghili and K. Parsa, "Motion and parameter estimation of space objects using laser-vision data," *Journal of Guidance, Control, and Dynamics*, vol. 32, no. 2, pp. 538–550, 2009.
- [16] M. Nayak, J. Beck, and B. Udrea, "Design of relative motion and attitude profiles for 3d rso imaging with a laser rangefinder," in *2013 IEEE Aerospace Conference*, 2013.
- [17] —, "Real-time attitude commanding to generate rso high density point clouds with a laser rangefinder," in *2013 IEEE Aerospace Conference*, 2013.
- [18] G. Boyarko, "Spacecraft guidance strategies for proximity maneuvering and close approach with a tumbling object," PhD, 2010.
- [19] G. Boyarko, Y. Oleg, and R. Marcello, "Real-time 6dof guidance for of spacecraft proximity maneuvering and close approach with a tumbling object," in *2010 AIAA/AAS Astrodynamics Specialist Conference*, ser. Guidance, Navigation, and Control and Co-located Conferences. AIAA, 2010.
- [20] G. Boyarko, O. Yakimenko, and M. Romano, "Optimal rendezvous trajectories of a controlled spacecraft and a tumbling object," *Journal of Guidance, Control, and Dynamics*, vol. 34, no. 4, pp. 1239–1252, 2011.
- [21] P. Patel, B. Udrea, and M. Nayak, "Optimal guidance trajectories for a nanosatellite docking with a tumbling resident space object," in *2015 IEEE Aerospace Conference*, 2015.
- [22] H. Prahlaad, R. Pelrine, S. Stanford, J. Marlow, and R. Kornbluh, "Electro-adhesive robots; wall climbing robots enabled by a novel, robust, and electrically controllable adhesion technology," in *2008 IEEE International Conference on Robotics and Automation (ICRA)*, 2008, pp. 3028–3033.
- [23] J. P. D. Tellez, J. Krahn, and C. Menon, "Characterization of electro-adhesives for robotic applications," in *IEEE International Conference on Robotics and Biomimetics (ROBIO)*, 2011, pp. 1867–1872.
- [24] W. Hongqiang, A. Yamamoto, and T. Higuchi, "Electrostatic-motor-driven electroadhesive robot," in *2012 IEEE/RSJ International Conference on Intelligent Robots and Systems (IROS)*, 2012, pp. 914–919.
- [25] W. Hongqiang and A. Yamamoto, "A thin electroadhesive inchworm climbing robot driven by an electrostatic film actuator for inspection in a narrow gap," in *2013 IEEE International Symposium on Safety, Security, and Rescue Robotics (SSRR)*, 2013, pp. 1–6.
- [26] T. Ryzhova, "Istc: Activity on space debris problem," in *IAF Symposium*, 2013.
- [27] Lockheed, "Shuttle/agency study," 1972.
- [28] M. Balas, S. Frost, and F. Hadaegh, "Evolving systems: A theoretical foundation," in *AIAA Guidance, Navigation, and Control Conference and Exhibit*, ser. Guidance, Navigation, and Control and Co-located Conferences. AIAA, 2006.
- [29] M. J. Balas and S. A. Frost, "An introduction to evolving systems of flexible aerospace structures," in *2007 IEEE Aerospace Conference*, 2007.
- [30] S. A. Frost and M. J. Balas, "Evolving systems: Adaptive key component control and inheritance of passivity and dissipativity," *Applied Mathematics and Computation*, vol. 217, no. 3, pp. 1034–1044, 2010.
- [31] S. Frost and M. Balas, "Evolving systems: An outcome of fondest hopes and wildest dreams," in *Guidance, Navigation, and Control Conference*, ser. Guidance, Navigation, and Control and Co-located Conferences. AIAA, 2012.
- [32] E. U. Firdaus, *Identification Of Stiffness Matrices Of*

*Structural And Mechanical Systems From Modal Data*. CRC Press, 2004.

- [33] J.-S. Lew, "Robust predictive control for structures under damage condition," *Journal of Guidance, Control, and Dynamics*, vol. 36, no. 6, pp. 1824–1829, 2013.
- [34] J. McCarthy, "Leostar-2 bus fact sheet," 2014.
- [35] "Ball aerospace configurable platforms," 2014.
- [36] S. Tietz, J. Bell, and B. Hine, "Multi-mission suitability of the nasa ames modular common bus," in *2009 Small-Sat Conference*, 2009.
- [37] R. Jakhu, "Active debris removal - an essential mechanism for ensuring the safety and sustainability of outer space," 2012.
- [38] B. Obama, "National space policy of the united states of america," 2010.
- [39] NASA, *Process for Limiting Orbital Debris (NASA-STD 8719.14)*. National Aeronautics and Space Administration, 2009.
- [40] E. A. Esther and C. Burnside, "Rs-34 (peacekeeper post boost propulsion system) orbital debris application concept study," in *2013 AIAA Space Conference and Exposition*, 2013.
- [41] J. R. Maly, V. M. Stavast, G. E. Sanford, and M. E. Evert, "Adapter ring for small satellites on responsive launch vehicles," in *7th Responsive Space Conference*, 2009.
- [42] J. Maly, "6u mount for cubesats on espa," in *9th CubeSat Annual Summer Workshop*, 2012.
- [43] G. Kehrl, "Athena mission planner's guide," 2012.
- [44] M. Steele and G. Kehrl, "Athena launch vehicle update," 2013.
- [45] "Network tactical (net-t) brochure," 2014.
- [46] R. Stechman, "Development and qualification of a 2nd generation 5 lbf (22n) bipropellant thruster," in *25th Joint Propulsion Conference*. AIAA, 1989.
- [47] —, "Development history of the 25 lbf (110 newton) space shuttle vernier thruster," in *26th Joint Propulsion Conference*. AIAA, 1990.
- [48] D. Petrick, "Application of spacecube in a space flight system," in *2009 Military and Aerospace Programmable Logic Devices Workshop*, 2009.
- [49] T. Flatley, "Advanced hybrid on-board science data processor spacecube 2.0," in *2011 American Geophysical Union Fall Meeting*, 2011.
- [50] "Canisterized satellite dispenser data sheet," 2013.
- [51] D. R. Defibaugh and G. Morrison, "Compressed liquid densities, saturated liquid densities, and vapor pressures of 1,1-difluoroethane," *Journal of Chemical and Engineering Data*, vol. 41, no. 3, pp. 376–381, 1996.
- [52] M. Lin, T. Flatley, A. Geist, and D. Petrick, "Nasa gsfc development of the spacecube mini," in *2011 SmallSat Conference*, 2011.
- [53] G. W. Hill, "Researches in the lunar theory," *American Journal of Mathematics*, vol. 1, no. 1, pp. 5–26, 1878.
- [54] T. Craychee and S. Sturtevant, "Mitigating potential orbital debris: The deorbit of a commercial spacecraft," in *2011 AAS/AIAA Astrodynamics Specialist Conference*, 2011.
- [55] M. Tillerson, "Coordination and control of multiple spacecraft using convex optimization techniques," Ph.D. dissertation, 2002.
- [56] M. Tillerson and J. P. How, "Advanced guidance algorithms for spacecraft formation-keeping," in *2002 American Control Conference*, 2002.
- [57] M. Baldwin, R. S. Erwin, and I. Kolmanovsky, "Robust controller for constrained relative motion maneuvering with disturbance rejection," in *Guidance, Navigation, and Control (GNC) Conference*. AIAA, 2013.
- [58] C. Wiedemann, S. Flegel, M. Moeckel, J. Gelhaus, V. Braun, C. Kebschull, J. Kreisel, M. Metz, and P. Vordersmann, "Cost estimation of active debris removal," in *63rd International Astronautical Congress*, 2012.
- [59] J. C. Bastante, A. Caramagno, L. F. Penin, J. Araujo, and B. Udrea, "Optimal guidance profiles for a formation flying demonstration missions in gto," in *AIAA Guidance Navigation and Control Conference and Exhibit*, 2005.
- [60] —, "Design of a formation flying demonstration mission in gto based on optimal guidance profiles," in *2005 International Astronautical Congress*, 2005.
- [61] D. Dumitriu, S. Marques, P. U. Lima, J. C. Bastante, J. Araujo, L. F. Penin, A. Caramagno, and B. Udrea, "Optimal guidance and decentralised state estimation applied to a formation flying demonstration mission in gto," *IET Control Theory and Applications*, vol. 1, no. 2, pp. 532–544, 2007.
- [62] T. Chabot and B. Udrea, "Xeus mission dynamics guidance and control," in *2006 AIAA Guidance, Navigation, and Control Conference and Exhibit*. AIAA, 2006.
- [63] C. Charbonnel, L. Pirson, F. Ankersen, and B. Udrea, "Accurate modes design of the darwin precursor formation flying demonstration mission," in *16th IFAC Symposium on Automatic Control in Aerospace*, 2004.
- [64] D. Dumitriu, S. Marques, P. U. Lima, and B. Udrea, "Decentralized, low-communication state estimation and optimal guidance of formation flying spacecraft," in *16th AAS/AIAA Space Flight Mechanics Meetings*, 2006.
- [65] B. Udrea and C. Decoust, "Relative navigation algorithm between cooperating spacecraft," in *Guidance Navigation and Control Conference and Exhibit*. AIAA, 2008.
- [66] L. Pirson, C. Charbonnel, B. Udrea, M. Rennie, P. McGuinness, and P. Palomo, "Darwin precursor demonstration mission: The icc2 study, from gnc design to real-time test bench validation," in *29th Annual AAS Rocky Mountain Guidance and Control Conference*, 2006.
- [67] DARPA, "Tactically expandable maritime platform (temp)," 2010.
- [68] J. C. Mankins, "Sps-alpha: The first practical solar power satellite via arbitrarily large phased array," NASA Innovative Advanced Concepts, Tech. Rep., 2012.
- [69] G. Ojakangas, P. Anz-Meador, and H. Cowardin, "Probable rotation states of rocket bodies in low earth orbit," in *2012 Annual Maui Optical and Space and Surveillance Technologies Conference*, 2012.
- [70] H. Cowardin, G. Ojakangas, M. Mulrooney, S. Lederer, and J.-C. Liou, "Optical signature analysis of tumbling rocket bodies via laboratory measurements," in *2012*

*Advanced Maui Optical and Space Surveillance Technologies Conference, 2012.*

- [71] N. Praly, "Rapport d'étude sur l'évaluation des couples de freinage par courant de foucault sur différentes géométries d'étage supérieur," SYSSNAV Navigation Solutions, Tech. Rep., 2012.
- [72] N. Praly, M. Hillion, C. Bonnal, J. Laurent-Varin, and N. Petit, "Study on the eddy current damping of the spin dynamics of space debris from the ariane launcher upper stages," *Acta Astronautica*, vol. 76, pp. 145–153, 2012.
- [73] C. Frueh and T. Schikdknecht, "Analysis of observed and simulated light curves of space debris," in *2010 International Astronautical Congress*, 2010.
- [74] A. A. Albuja, D. J. Scheeres, and J. W. McMahon, "Evolution of angular velocity for space debris as a result of yorp," *Advances in the Astronautical Sciences*, 2013.
- [75] J.-C. Liou, "Active debris removal activities at the nasa orbital debris program office," 2012.
- [76] S. Kar, J. M. F. Moura, and K. Ramanan, "Distributed parameter estimation in sensor networks: Nonlinear observation models and imperfect communication," *IEEE Transactions on Information Theory*, vol. 58, no. 6, pp. 3575–3605, 2012.
- [77] S. Kar and J. M. F. Moura, "Convergence rate analysis of distributed gossip (linear parameter) estimation: Fundamental limits and tradeoffs," *IEEE Journal of Selected Topics in Signal Processing*, vol. 5, no. 4, pp. 674–690, 2011.
- [78] S. Kar, C. Shuguang, H. V. Poor, and J. M. F. Moura, "Convergence results in distributed kalman filtering," in *2011 IEEE International Conference on Acoustics, Speech and Signal Processing (ICASSP)*, 2011.
- [79] J. Nelson, M. Balas, and R. Erwin, "Model reference adaptive control of linear systems with time varying input/output delays," in *Guidance, Navigation, and Control Conference*, ser. Guidance, Navigation, and Control and Co-located Conferences. AIAA, 2012.
- [80] S. Frost and M. Balas, "Adaptive key component controllers for evolving systems," in *2008 AIAA Guidance, Navigation and Control Conference and Exhibit*, ser. Guidance, Navigation, and Control and Co-located Conferences. AIAA, 2008.
- [81] T. Lips and B. Fritsche, "A comparison of commonly used re-entry analysis tools," *Acta Astronautica*, vol. 57, no. 28, pp. 312–323, 2005.

## BIOGRAPHY



**Bogdan Udrea** received his Dipl.Eng. in Aeronautical Engineering from the Polytechnic Institute of Bucharest, Romania in 1990 and his Ph.D. in Aeronautics and Astronautics from the University of Washington in 1999. He is the founder and CEO of VisSidus Technologies, Inc., a company that develops technologies for outer space sustainability. Bogdan has a day job as an Associate Professor of Aerospace Engineering at the Embry-Riddle Aeronautical University and has previously worked as a Control and Navigation Systems Engineer at the European Space Agency. His

research interests include spacecraft dynamics and control and space mission design with emphasis on proximity operations, formation flying, near-Earth object exploration and on-board autonomy.



**Michael (Mikey) Nayak** received a B.S. and M.S. in Aerospace Engineering from Embry-Riddle Aeronautical University, Daytona Beach, FL. He is currently pursuing a Ph.D. degree in Earth and Planetary Science at the University of California, Santa Cruz. He is also an active duty Air Force officer, the Chief Scientist of the ARAPAIMA Program, and founder of the aerospace consulting firm Red Sky Research, LLC. Mikey has served as Lead Flight Director and Mission Manager for the Air Force Research Laboratory's Tactical Satellite-III and has managed operations for the NASA Earth Science pathfinder CloudSat. He is the recipient of a National Defense Science and Engineering Graduate (NDSEG) Fellowship and the 2013 General Samuel C. Phillips award for the Space and Missile System Centers Outstanding Young Engineer/Scientist.